Sodium manganese fluorosulphate with a triplite structure

Authors

Prabeer Barpanda[ab]*, Chris D Ling[c], Gosuke Oyama[a] and Atsuo Yamada[ab]

[a]Department of Chemical System Engineering, The University of Tokyo, 7-3-1 Hongo, Bunkyo-ku, Tokyo, 113-8656, Japan
[b]Unit of Elements Strategy Initiative for Catalysts & Batteries (ESICB), Kyoto University, Kyoto, 615-8510, Japan
[c]School of Chemistry, The University of Sydney, Building F11, Sydney, NSW, 2006, Australia

Correspondence email: prabeer@chemsys.t.u-tokyo.ac.jp

Synopsis The crystal structure of $NaMnSO_4F$ fluorosulphate compound has been solved, refined and compared with other alkali metal fluorosulphates and naturally occurring triplite-type minerals.

Abstract The crystal structure of the $NaMnSO_4F$ fluorosulphate phase prepared by low-temperature solid-state synthesis has been solved and refined by the Rietveld analysis of synchrotron X-ray powder diffraction data. Isostructural to the naturally occurring *triplite* family of minerals, this compound crystallizes in monoclinic $C2/c$ symmetry (#15) with unit cell parameters of a = 13.77027(17), b = 6.63687(8), c = 10.35113(14) Å, β = 121.4795(3)° and V = 806.78(2) Å^3. Its structure is built of edge-sharing chains of distorted MO_4F_2 octahedra, which are interconnected by constituent SO_4 tetrahedra to form a robust three-dimensional polyanionic framework. MO_4F_2 octahedra are randomly occupied by Na and Mn with close to 1:1 occupancy. This random mixing of cations among polyhedral building blocks means that there are no channels for Na-ion conduction, rendering it electrochemically inactive. The structure is discussed and compared to other known alkali metal fluorosulphates as well as to naturally occurring triplite-type minerals.

Keywords: sodium-ion battery cathodes; fluorosulphates; $NaMnSO_4F$; triplite; disorder.

1. Introduction

In the search for novel high-voltage polyanionic cathode materials to rival triphylite-type $LiFePO_4$ (Padhi *et al.*, 1997), the chemistry of metal fluorosulphates $A^{I}M^{II}SO_4F$ (A = alkali metal Li/ Na/ K, M = divalent 3d metals) has been widely explored. This has led to the discovery of a large family of polyanionic insertion materials, the first being tavorite-type $LiFeSO_4F$ (Recham *et al*., 2010; Tarascon *et al*., 2010). Isostructural to $LiMgSO_4F$ (Sebastian *et al.*, 2002), the $LiFeSO_4F$ compound was found to be an excellent low-cost, high-performance cathode material delivering a reversible capacity of ~140 mAh/g at 3.6 V (vs. Li/Li$^+$). The following three years witnessed the discovery of a whole family of novel $LiMSO_4F$ (M = Co, Ni, Mn, Zn) compounds (Barpanda *et al.*, 2010, 2011). They

display extensive polymorphism and promising electrochemical properties, notably the highest Fe^{3+}/Fe^{2+} redox activity at 3.9 V ever reported (Ati *et al.*, 2011; Barpanda *et al.*, 2011).

The exploration of fluorosulphate compounds was successfully extended to sodium-based Na*M*SO_4F (Ati *et al.*, 2010; Barpanda *et al.*, 2010; Reynaud *et al.*, 2012) and potassium-based K*M*SO_4F (Recham *et al*., 2012) homologues. While many Li-based and K-based fluorosulphates turned out to be efficient insertion materials suitable for battery applications, none of the Na-based fluorosulphates was found to be electrochemically active owing to high activation energy barriers and structural limitation (Tripathi *et al*., 2011). Despite this massive synthetic electrochemical and crystallographic effort, the structure of $NaMnSO_4F$ remained unknown. This is a significant oversight, because the structure of alkali metal fluorosulphate can vastly alter with different size of constituent 3*d* metals and alkali cations. Here, we report that the crystal structure of $NaMnSO_4F$ adopts the triplite-type mineral structure. The structural details are described in comparison to other known *AM*SO_4F compounds and correlated to its electrochemical limitations.

2. Experimental

2.1. Low temperature synthesis

The target fluorosulphate compound, $NaMnSO_4F$, was prepared by classical solid-state synthesis. Stoichiometric amounts of NaF (Wako, 99 %) and *szomolnokite*-structured $MnSO_4.H_2O$ monohydrate (Alfa Aesar, 97 %) precursors were intimately mixed by a shaker-type milling unit (TKMAC 1200, Topologic System Inc.) for 1 h (400 rpm) employing stainless steel milling media and container. This mixture was pressed into cylindrical pellets by applying 10 MPa of uniaxial pressure. These pellets were loaded into a Teflon-lined Parr reactor under ambient atmosphere and annealed at 295 °C for 30-48 h (heating rate = 5 °C/ min). The dehydration of the monohydrate precursor generates an autogeneous pressure inside the Parr reactor controlling the reaction kinetics of progressive dehydration and product formation. The net reaction can be expressed as:

$$NaF(s) + MnSO_4.H_2O\ (s) \rightarrow NaMnSO_4F\ (s) + H_2O\ (g)\uparrow$$

The sintered pellets (milky white colour) were ground by mortar and pestle for further analyses. Alternatively, dehydrated $MnSO_4$ can be reacted with NaF at higher temperature (500-550 °C) for 10-12 h under inert atmosphere to obtain $NaMnSO_4F$ product. All further material analyses were performed on the $NaMnSO_4F$ sample prepared using the low temperature (ca. 295 °C) procedure.

2.2. Data collection, structure solution and refinement

A synchrotron X-ray powder diffraction (XRD) pattern of a polycrystalline $NaMnSO_4F$ powder sample was acquired at the Powder Diffraction (PD) beamline of the Australian Synchrotron, at a wavelength of λ = 0.58966 Å, calibrated against a LaB_6 standard (NIST SRM660a). A finely ground

sample was placed in a sealed 0.3mm diameter glass capillary that was rotated during the measurements. Rietveld refinement (Rietveld, 1969) and structure analysis were performed using the GSAS software package (Larson & Von Dreele, 1994) with the EXPGUI front-end (Toby, 2001), against data over the 2θ range 5.6–55 °. A *C*-centred monoclinic unit cell was identified, from which a reduced unit cell search of the Inorganic Crystal Structure Database yielded triplite-type $LiMnSO_4F$ with monoclinic *C*2/*c* symmetry (#15) (Rea & Kostiner, 1972) as the first result, at a 3% tolerance. This phase was used as the basis for a starting model of $NaMnSO_4F$. Fractional atomic coordinates for all atoms could be freely refined, along with isotropic atomic displacement parameters (ADPs) and fractional occupancies on the mixed Na/Mn sites (constrained to fix the total composition at $NaMnSO_4F$). Refinement details are presented in **Table 1**, with selected bond lengths in **Table 2**. The structure is illustrated in **Figure 2**.

The morphology of the as-obtained product mounted on conducting carbon paste was observed with a Hitachi S-4800 SEM unit operating at 1.5 kV. Infra-red spectrum was collected with a JASCO FT/IT-6300 FTIR instrument over 400 – 4000 cm^{-1} with a step size of 4.0 cm^{-1}. Thermal analysis (TGA) was conducted with a Seiko EXSTAR 6000 unit in the temperature range of 25 – 600 °C (heating rate = 5 °C/min). $NaMnSO_4F$ powder was later tested for possible electrochemical activity. A composite mixture of $NaMnSO_4F$, conducting carbon and polyvinylidene difluoride (PVdF) binder (in w/w ratio of 70/20/10) was used as working electrode and tested in standard half-cell architecture using Na metal as the counter electrode and 1 M $NaClO_4$ dissolved in propylene carbonate as the electrolyte. The cells were galvanostatically cycled between 2 ~ 4.5 V at rate of C/20 (at 25 °C).

3. Results and discussion

The fluorosulphate family of compounds can be obtained by various non-aqueous soft-chemistry routes owing to their high tendency for dissolution and thermal decomposition. The present study used a topotactic dual ion-exchange route to obtain $NaMnSO_4F$ by simultaneous exchange of OH^- by F^- and H^+ by Na^+. This soft chemical approach enabled a low reaction temperature (T_r = 295 °C) with rather slow kinetics, permitting a pure sample of $NaMnSO_4F$ to be obtained for the first time. Large micrometric agglomerates consisting of nanoscale (50-200 nm) secondary particles with spherical morphology were observed (supplementary information, **Figure S1**). The final Rietveld-refined fit to experimental XRD data, shown in **Figure 1**, confirms the near-perfect phase purity of the sample. A small number of weak and relatively broad peaks remain unindexed, indicating the presence of a poorly crystalline impurity phase(s) that could not be identified. However, given the extremely weak nature of these peaks (the strongest of which has 1% the intensity of the strongest main phase peak) we are confident that they do not significantly compromise our refinement of $NaMnSO_4F$.

$NaMnSO_4F$ belongs to triplite family of compounds isostructural to triplite minerals Mn_2PO_4F or $(Mn,Fe,Mg,Ca)_2PO_4(F,OH)$ (Rea & Kostiner, 1972). The triplite-type structure can be described as a

close-packed ensemble of MO_4F_2 octahedral units arranged in a edge-sharing fashion to form two crystallographically distinct chains along the [101] and [010] directions. The two crystallographically distinct *M* sites are occupied by Na and Mn in an almost random statistical distribution; in this sense, it can be considered a disordered derivative of the tavorite family of fluorosulphates. In contrast to tavorite (Yakubovich & Urusov, 1997), however, in $NaMnSO_4F$ the MO_4F_2 octahedra have constituent F atoms in *cis* positions. The presence of more electronegative F atoms in one side and less electronegative O atoms in other side of central Mn atom leads to octahedral distortion. The distortion (Δ) of MnO_4F_2 octahedral units can be quantified as:

$$\Delta = \frac{1}{6}\sum_{n=1}^{6}\left\{\frac{(dn - \langle d\rangle)}{\langle d\rangle}\right\}^2$$

where, *dn* and $\langle d\rangle$ are individual Mn–O/Mn–F bond length and mean bond length respectively. In the case of $NaMnSO_4F$, the distortion (Δ) value was calculated to be ~10 ($\times 10^{-4}$), which is smallest among the family of Na*M*SO_4F (*M* = Fe, Co, Mg, Cu. Zn) having Δ values in the range 23–110 ($\times 10^{-4}$) (Reynaud *et al.*, 2012). These tavorite-structured Na*M*SO_4F homologues having MO_4F_2 octahedra exclusively connected by corner-sharing of F atoms located in *trans* positions, thus retains a large degree of distortion. However, triplite-structured $NaMnSO_4F$ has neighbouring MnO_4F_2 octahedra connected by edge-sharing of O–O, F–F or O–F atoms, which reduces the octahedral distortion. These chains of distorted MO_4F_2 are in turn connected by corner-sharing with SO_4 tetrahedra to develop an overall three-dimensional polyanionic framework. The accuracy of this triplite structure was verified by bond valence sum (BVS) calculation using the formula: $BVS = \sum \exp\left[(d_0 - di)/B\right]$, where d_i is the bond length between neighbouring cation-anion pairs. The parameter d_0 and B = 0.37 are empirically determined for specific cation-anion pairs (Brown, 1992; Brown & Altermatt, 1985). The BVS values for metal atoms are included in Table 2, and indicate that this part of the structure suffers from significant local strain: Mn1 and Mn2 are significantly underbonded compared to their expected valence of 2, with calculated BVS of 1.662(6) and 1.442(5) respectively; while Na1 and Na2 are significantly overbonded compared to their expected valence of 1, with calculated BVS of 1.673(6) and 1.449(5) respectively. Despite this, our diffraction data contained no evidence for Na/Mn ordering that might resolve this strain, and the occupancies of *M*1 and *M*2 refined to an almost perfectly random distribution on both sites. A random distribution model, which contains no channels for alkali ion migration, is also supported by the fact that our electrochemical measurements revealed no evidence for significant electrochemical activity (supplementary information, **Figure S2**). Similar electrochemical inactivity has been earlier noticed for triplite $LiMnSO_4F$. However, in the latter case, isostructural substitution of Mn by Fe alters the degree of occupancy in *M*1 and *M*2 site to create a pseudo-zig-zag channels for Li^+-ion mobility, making it suitable as a cathode material (Barpanda *et*

al., 2011). Using the same strategy, synthesis of triplite-structured $NaFeSO_4F$ may well lead to a novel candidate for sodium-ion batteries.

The structure of $NaMnSO_4F$ was further probed with infrared spectroscopy. As shown in **Figure 3**, the resulting spectra consist of two sets of peaks. The broad peak ~3500 cm^{-1} can be convoluted to two peaks linked to symmetric stretching (at 3450 cm^{-1}) and asymmetric stretching (at 3615 cm^{-1}) of OH^- groups, which can arise from the slight amount of unreacted $MnSO_4.H_2O$ monohydrate precursor or surface moisture contamination of $NaMnSO_4F$ product. The signature peaks at lower wavenumbers corresponds to the SO_4^{2-} building blocks. Four distinct peaks are observed owing to stretching modes of SO_4^{2-}: (i) symmetric stretching (ν_1 ~ 983 cm^{-1}) and (ii) asymmetric stretching mode (ν_3 ~ 1105 cm^{-1}) and bending mode of SO_4^{2-}: (iii) symmetric bending (ν_2 ~ 450 cm^{-1}) and (ii) asymmetric bending mode (ν_4 ~ 611 cm^{-1}). In the current triplite structure, the SO_4 tetrahedra are very slightly asymmetric owing to interconnecting distorted MO_4F_2 octahedral units, having S–O bonds of 1.480, 1.474, 1.463 and 1.491 Å. This differential bond lengths in SO_4^{2-} tetrahedra trigger degeneration of all stretching and bending vibrational peaks so as to form broad and asymmetric vibrational bands as marked in **Figure 3** (Nakamoto, 1986).

Finally, the thermal and chemical stability of $NaMnSO_4F$ was measured. The fluorosulphate family of compounds, in general, suffers from low thermal stability owing to the weaker S–O bonds vis-à-vis the stronger phosphate (P–O) group of compounds. While majority of fluorosulphate members starts decomposing over 350 °C, $NaMnSO_4F$ was found to be thermally stable up to 600 °C (**Figure 4**). This can be explained by the non-reactive nature of Mn and the large exchange energy gain in the d^5 electronic configuration of Mn^{2+} state in $NaMnSO_4F$. However, owing to moisture-sensitive SO_4^{2-} and F^- components, it was found to dissolve completely in water, as is typical for SO_4-based compounds.

4. Conclusions

In this work, the phase-pure $NaMnSO_4F$ fluorosulphate compound was prepared by low-temperature solid-state reaction and its crystal structure has been solved and refined using the Rietveld method against X-ray powder diffraction data. Its structure is distinct from previously reported $NaMSO_4F$ tavorite-type compounds. $NaMnSO_4F$ adopts a monoclinic framework, falling into the *triplite* type, with intertwined chains of edge-sharing MO_4F_2 octahedral units joined together by SO_4 tetrahedral units. It can be defined as a disordered and thermodynamically stable version of the tavorite structure, where the alkali species (Na^+ and Mn^{2+}) statistically occupy the same sites with large six-fold coordination. This disorder means that the compound lacks continuous ion-conducting channels, rendering it electrochemically inactive. Nevertheless, $NaMnSO_4F$ represents a new member of the structurally diverse fluorosulphate family, and knowledge of its synthesis and structure contribute to the understanding of these potentially technologically important compounds.

Acknowledgements This work was partly supported by 'Element Strategy Initiative for Catalysts & Batteries (ESICB)' program by the Ministry of Education, Culture, Sports, Science and Technology (MEXT). The first author (PB) acknowledges the Japan Society for the Promotion of Science (JSPS) for a JSPS Fellowship at the University of Tokyo. The second author (CDL) is grateful to Australian Research Council for financial support (DP110102662) and to Dr Peter Blanchard for collecting synchrotron X-ray diffraction data.

References

Ati, M., Dupont, L., Recham, N., Chotard, J. N., Walker, W. T., Davoisne, C., Barpanda, P., Sarou-Kanian, V., Armand, M. & Tarascon, J. M. (2010). *Chem. Mater.* **22**, 4062-4068.

Ati, M., Melot, B. C., Rousse, G., Chotard, J. N., Barpanda, P. & Tarascon, J. M. (2011). *Angew. Chem. Int. Ed.* **50**, 10574-10577.

Barpanda, P., Recham, N., Chotard, J. N., Djellab, K., Walker, W., Armand, M. & Tarascon, J. M. (2010). *J. Mater. Chem.* **20**, 1659-1668.

Barpanda, P., Chotard, J. N., Recham, N., Delacourt, C., Ati, M., Dupont, L., Armand, M. & Tarascon, J. M. (2010). *Inorg. Chem.* **49**, 7401-7413.

Barpanda, P., Chotard, J. N., Delacourt, C., Reynaud, M., Filinchuk, Y., Armand, M., Deschamps, M. & Tarascon, J. M. (2011). *Angew. Chem. Int. Ed.* **50**, 2526-2531.

Barpanda, P., Ati, M., Melot, B. C., Rousse, G., Chotard, J. N., Doublet, M. L., Sougrati, M., Corr, S. A., Jumas, J. C. & Tarascon, J. M. (2011). *Nat. Mater.* **10**, 772-779.

Brown, I. D. (1992). *Acta Cryst. B.* **48**, 553-572.

Brown, I. D. & Altermatt, D. (1985). *Acta Cryst. B.* **41**, 244-247.

Larson, A. C. & Von Dreele, R. B. (1994). *Los Alamos National Laboratory Report* LAUR 86-748.

Nakamoto, K. (1986) *Infrared and Raman Spectra of Inorganic and Coordination Compounds.* Wiley Pub.

Padhi, A. K., Nanjundaswamy, K. S. & Goodenough, J. B. (1997). *J. Electrochem. Soc.* **144**, 1188-1194.

Rea, J. R. & Kostiner, E. (1972) *Acta Cryst. B.* **28**, 2525-2529.

Recham, N., Chotard, J. N., Dupont, L., Delacourt, C., Walker, W., Armand, M. & Tarascon, J. M. (2010). *Nat. Mater.* **9**, 68-74.

Recham, N., Rousse, G., Sougrati, M. T., Chotard, J. N., Frayret, C., Mariyappan, S., Melot, B. C., Jumas, J. C. & Tarascon, J. M. (2012). *Chem. Mater.* **22**, 4363-4370.

Reynaud, M., Barpanda, P., Rousse, G., Chotard, J. N., Melot, B. C., Recham, N. & Tarascon, J. M. (2012) *Solid State Sci.* **14**, 15-20.

Rietveld, H. M. (1969) *J. Appl. Cryst.* **2**, 65-71.

Sebastian, L., Gopalakrishnan, J. & Piffard, Y. (2002). *J. Mater. Chem.* **12**, 374-377.

Tarascon, J. M., Recham, N., Armand, M., Chotard, J. N., Barpanda, P., Walker, W. & Dupont, L. (2010). *Chem. Mater.* **22**, 724-739.

Toby, B. H. (2001). *J. Appl. Cryst.* **34**, 210-213.

Tripathi, R., Gardiner, G. R., Islam, M. S. & Nazar, L. F. (2011) *Chem. Mater.* **23**, 2278-2284.

Yakubovich, O. V. & Urusov, V. S. (1997). *Geochem. Int.* **35**, 630-638.

Table 1 Details of the Rietveld refinement against X-ray powder diffraction data of $NaMnSO_4F$.

Formula/ Molecular weight (M_r)	$NaMnSO_4F$ / 192.989
Cell setting, space group (No.)	Monoclinic, *C*2/*c* (#15)
Unit cell parameters: *a*, *b*, *c* (Å)	13.77027(17), 6.63687(8), 10.35113(14)
β (°)	121.4795(3)
Vol (Å^3)	806.78(2)
Z	8
Density (D_x, g.cm^{-3})	3.17779(8)
Specimen form, colour	Polycrystalline powder, milky white
Background function	Shifted Chebyshev as implemented in GSAS (function #1)
Profile function	Pseudo-Voigt as implemented in GSAS (function #2)
R-factors	Rp = 0.0369, Rwp = 0.0480, $R(F^2)$ = 0.04073
Goodness-of-fit	2.17
Number of refined variables	61

Table 2 Selected interatomic distances *d* (Å) and metal atom bond valence sums (BVS) from the Rietveld-refined structure of $NaMnSO_4F$.

*M*1–O(2)	2.221(3)	*M*2–O(1)	2.354(3)	S–O(1)	1.480(3)
*M*1–O(3)	2.252(3)	*M*2–O(1)	2.312(3)	S–O(2)	1.474(2)
*M*1–O(4)	2.217(3)	*M*2–O(2)	2.291(3)	S–O(3)	1.463(3)
*M*1–O(4)	2.374(3)	*M*2–O(3)	2.320(3)	S–O(4)	1.491(3)
*M*1–F	2.142(2)	*M*2–F	2.149(2)		
*M*1–F	2.225(2)	*M*2–F	2.317(3)		
Average = 2.238		Average = 2.289		Average = 1.477	

BVS(Na1) = 1.673(6) BVS(Na2) = 1.449(5)

BVS(Mn1) = 1.662(6) BVS(Mn2) = 1.442(5)

Both *M*1 and *M*2 sites are partially occupied by Na and Mn.

Figure 1 Final Rietveld-refined fit of the structure of $NaMnSO_4F$ to synchrotron X-ray powder diffraction data (λ = 0.58966 Å) showing the experimentally observed (red crosses), calculated (upper line), difference (lower line) and Bragg diffraction positions (ticks). Data in the region 25–55 °2θ are shown above with the intensity scale magnified by a factor of 50.

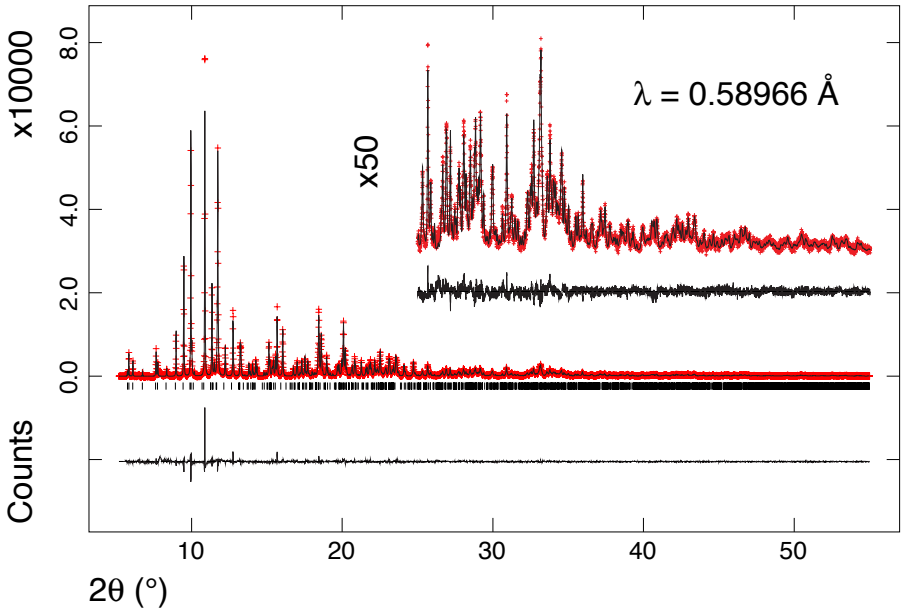

Figure 2 (a) Polyhedral representation of the final Rietveld-refined structure of $NaMnSO_4F$, showing interconnected edge-sharing MnO_4F_2 octahedra (purple) and corner-sharing SO_4 tetrahedra (yellow). Oxygen atoms are red and fluorine atoms are green. (b) Expanded view of part of the structure, showing the coordination environments of *M*1, *M*2 and *S*. The occupancies of mixed *M*1 and *M*2 sites are indicated by dividing the spheres into purple (Mn) and grey (Na).

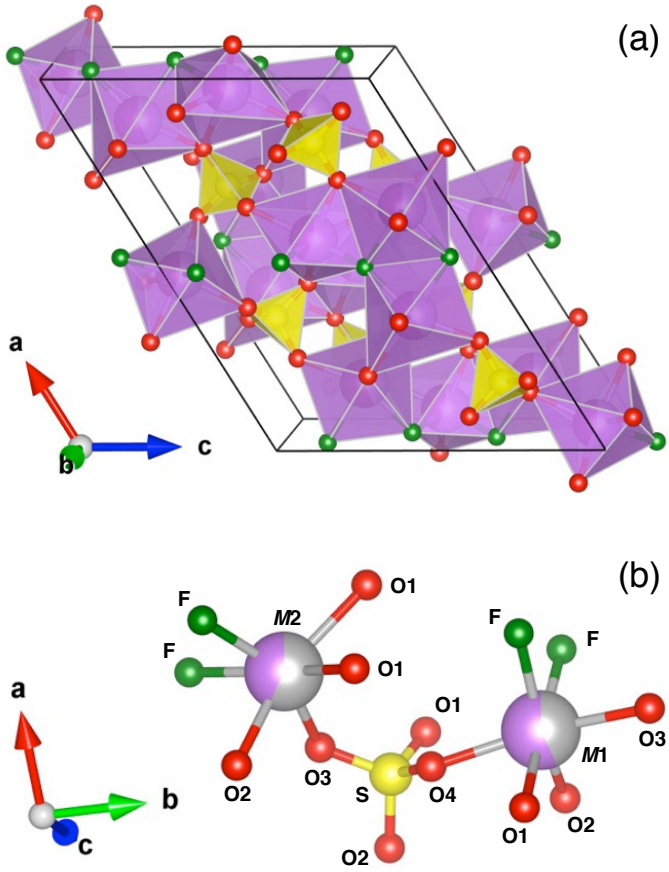

Figure 3 FT-Infra red spectrum of $NaMnSO_4F$ showing distinct vibration bands resulting from constituent SO_4 building blocks.

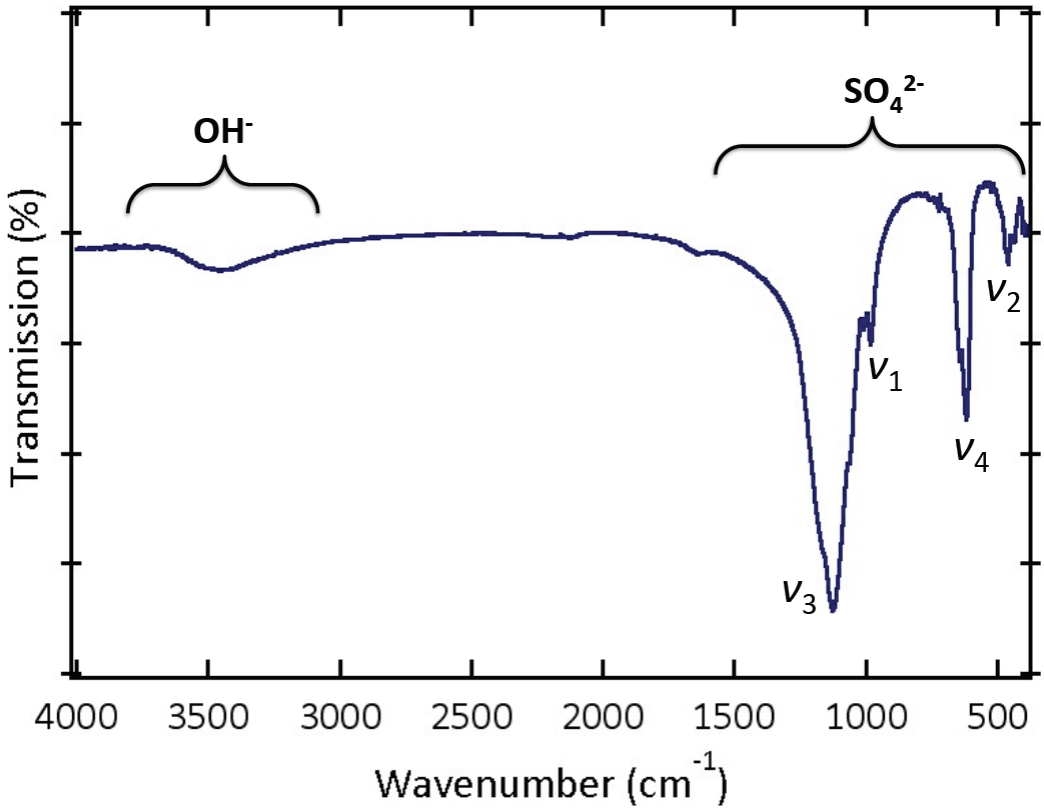

Figure 4 Thermogravimetric analysis (TGA) of $NaMnSO_4F$ conducted up to 600 °C, showing no weight change during heating and cooling segments.